Journal of Colloid and Interface Science 345 (2010) 214–221

Contents lists available at ScienceDirect

Journal of Colloid and Interface Science

www.elsevier.com/locate/jcis

Surface characterization of functionalized latexes with different surface functionalities using rheometry and dynamic light scattering

Jan S. Vesaratchanon [a], Koichi Takamura [b], Norbert Willenbacher [a,*]

[a] Institute of Mechanical Process Engineering and Mechanics, Karlsruhe Institute of Technology, Gotthard-Franz-Str. 3, 76131 Karlsruhe, Germany
[b] BASF Corporation, Charlotte Technical Center, Charlotte, NC, USA

ARTICLE INFO

Article history:
Received 19 November 2009
Accepted 6 February 2010
Available online 13 February 2010

Keywords:
Carboxylated latex
High frequency rheology
Electrosteric stabilization
Colloidal dispersion
Dispersion stability

ABSTRACT

Here we study the formation of sterically stabilizing "hairy" surface layers for a series of styrene–butylacrylate and styrene–butadiene latexes copolymerized either with acrylic acid (AA), methacrylic acid (MAA), itaconic acid (IA) or acrylamide (AM) using dynamic light scattering, steady shear and high frequency rheology. This phenomenon is investigated under different conditions of pH, ionic strength, and temperature. The AA copolymerized latex has the most extended hairy layer and is very sensitive to pH and ionic strength. MAA yields a thinner hairy layer than AA due to higher hydrophobicity. IA exhibits a hairy layer thickness of about 1 nm, since it terminates polymer chain growth. For the AM copolymerized latexes high frequency viscosity reveals the existence of a thin hairy layer and the high values of the low shear viscosity and the high frequency modulus are attributed to a weak, reversible flocculation. No significant effect of particle core composition or temperature on the formation of the hairy layer was observed. High frequency rheology is most valuable for characterization of surface layers of carboxylated latexes, since it provides not only direct information about the effective volume fraction but also characterizes the strength of colloidal interactions among particles and it is applied at high particle concentration relevant during manufacturing and processing.

1. Introduction

Carboxylated latex dispersion provide a cost-effective basis for the formulation of a large number of consumer products, including adhesives, paints, coatings, carpet-backing, texture modifications, etc. A carboxylated latex consists of a latex particle core with a polymer brush on the particle surface that could be produced by chemically grafting of functional polymers or by introducing functional co-monomers during polymerization [1–5] (Fig. 1). The key goal of using carboxylated latexes is to enhance dispersion stability during manufacturing and processing since the polymer brush, often termed "hairy" surface layer, provides steric repulsion among particles and improves the stability of filler-latex systems in complex formulations. Finally, it also improves the mechanical strength of dried latex films [6].

It is well-known that the carboxyl layer dissociates upon increasing the serum pH (typical values for pKa ~4.5 for acrylic and methacrylic acid while itaconic acid has two-step dissociation with pKa of ~3.85 and 5.5). This increases the solubility of the copolymer on the particle surface resulting in a swollen "hairy" surface layer. Since the degree of swelling also depends on electrostatic interaction among carboxyl groups, the thickness of the hairy layer depends on ionic strength of the serum. Ortega-Venuesa et al. [7] reported that electrosterically stabilized polystyrene particles are sensitive to the background ionic strength. Their results could be explained by classical DLVO theory where the importance of the electrosteric effect needed to be properly incorporated into the model including the thickness of the surface layer. Romero-Cano et al. [8] reported that the stability of carboxylated polystyrene dispersion increased monotonically upon increasing pH from 5 to 10, clearly due to the dissociation of the carboxyl groups. Reynhout et al. [9] reported that the dispersion stability of polystyrene latex particles is improved when acrylic acid is introduced, particularly at high ionic strength beyond the critical coagulation concentration of the bare polystyrene latex. Guo and Ballauff [10,11] investigated the effect of KCl salt on the hydrodynamic radius of polystyrene particles with (poly)acrylic acid grafted onto the surface with brush thickness, L on the same order of magnitude as the core particle radius a. They used dynamic light scattering to characterize the thickness of the acrylic acid layer, directly showing the swelling of the brush with increasing pH and a monotonic shrinkage with increasing ionic strength (at constant pH). Fritz et al. [12] studied the limit of thin surface layers ($L \ll a$) grafting short methacrylic acid chains ($M_w \sim 7000$ g/mol) onto styrene–n-butylacrylate core particles ($a = 53$ and 68 nm). They determined L for different pH and ionic strength from dynamic light scattering

* Corresponding author. Fax: +49 721 608 3758.
E-mail addresses: Norbert.Willenbacher@kit.edu, Sudaporn.Vesaratchanon@kit.edu (N. Willenbacher).

0021-9797/$ - see front matter © 2010 Elsevier Inc. All rights reserved.
doi:10.1016/j.jcis.2010.02.013

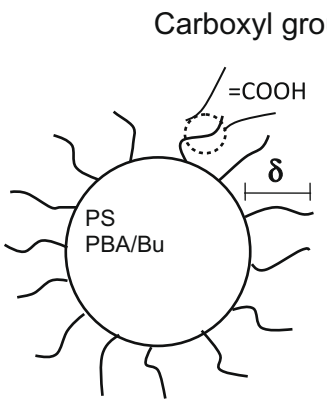

Fig. 1. Carboxylated latex particles with a core of polystyrene–butylacrylate or polystyrene butadiene copolymer. The hairy layer on the surface results from the dissociation of the carboxyl group as pH of the serum increases, hair length, δ varies with pH and ionic strength of the serum.

(DLS), zero shear and high frequency viscosity measurements and quantified the strength of steric repulsion based on high frequency storage modulus. Technically relevant carboxylated latexes are from copolymerization of functional co-monomers with the main monomers during emulsion polymerization rather than by grafting of appropriate polymer brushes. The distribution of these functional monomers among particle core surface and liquid phase is not known a priori and strongly depends on the choice of the monomers and polymerization conditions. Nevertheless, such systems are of outstanding technical and commercial importance and require improved characterization, especially under concentrated conditions.

High frequency rheology provides a great benefit to the understanding of the surface properties of such complex particle systems. In the high frequency regime, the applied oscillatory shear field characterized by its angular frequency ω, is much faster than the Brownian motion of the particles, i.e. $a^2\omega/D_s \gg 1$ where D_s denotes the self-diffusivity of the particles. On the other hand the solvent molecules are in phase with the external shear field. Accordingly, hydrodynamic interactions determine the high frequency viscosity, whereas the colloidal interactions show up in the out-of-phase signal, the storage modulus G'. Since deformation is small, the equilibrium structure of the dispersion, including the hairy layer, can be considered. For aqueous dispersions the appropriate frequency range is on the order of $\omega > 1000\ s^{-1}$.

Considerable research efforts have been spent during the past decades to study the surface properties of carboxylated latex dispersions. However, the progress has been rather slow. Classical electro-kinetic experiments are difficult to interpret due to the complex structure of the particle surface. Rheological measurements have provided great benefit in characterization of surface properties of electrosterically stabilized dispersions along with the development of elaborate statistical mechanical theories taking into account hydrodynamic interactions, equilibrium particle distribution as well as colloidal interactions [12–15].

Here, we apply high-frequency rheometry, steady shear and dynamic light scattering techniques to characterize latex particles functionalized with different "hairy" surface layers. These include latexes carboxylated with acrylic acid, methacrylic acid and itaconic acid as well as acrylamide (electrically neutral latex). Both styrene–butylacrylate and styrene–butadiene latexes with the same degree of the functionalization are compared in this study. The effect of serum pH, ionic strength and temperature on the rheological properties is investigated.

2. Experimental procedure

2.1. Latex systems

Seven latexes with different monomer mixtures were made using classical emulsion polymerization. Acrylic acid, methacrylic acid, itaconic acid as well as acrylamide were used as functional co-monomers at a level of 2 wt.% relative to the total monomer concentration. In one set of samples styrene and butylacrylate (1:1.1 mixing ratio) were used as main monomers (BASF SE, Ludwigshafen, Germany). Styrene–butadiene latexes in a second series were prepared with the same degree of functional co-monomers (BASF Corp., Charlotte, NC, USA). The particle size of all latexes is ~180 nm in diameter (controlled by seed polymerization) except for the polystyrene-butadiene latex with acrylic acid which has the diameter of 250 nm. The glass temperature, T_g of all latexes studied here is 10 °C. After polymerization the dispersions were dialyzed against deionized water in order to remove the electrolytes, surfactants and oligomers from the serum remaining from the synthesis. Here, our dialysis setup allowed the distilled water flow through the dialysis membrane (Carl Roth GmbH, Molecular weight cut off limit: 4000–6000 g/mol), which was immersed in the container filled with latex dispersion. The exit distilled water would drain out through another end of the membrane. During dialysis procedure, the electrolytes in the latex dispersion would flow into the membrane and drain out at the exit. The flow rate of the distilled water was controlled by attaching a small valve at the exit. The decrease of the dispersion conductivity with time indicated that the electrolytes were removed from the dispersion. The limited volume of the container prevents the dilution of the latex with distilled water. Dialysis procedure was carried out until the conductivity of the dispersion and the exit water remained unchanged with time, i.e. an equilibrium stage was reached. In this case the dispersion pH has changed from 1.8 to 2.5 whereas the conductivity dropped from 5 mS to 0.9 mS after about 15 days. After that the pH was adjusted by adding 10 M NaOH solution until the desired pH was reached. Series of concentrations were prepared by dilution with deionized water.

2.2. Dynamic light scattering measurement (DLS)

Dynamic light scattering measurements were performed using a Beckman Coulter (Model: N4 Plus) device. All measurements were carried out under dilute conditions (between 10^4 and 10^6 counts per second). The wavelength of 658 nm was used with a scattering angle of 90°. All samples were prepared with an ionic strength controlled by an addition of 1:1 NaCl salt to achieve the desired values (of 10 and 100 mM). After that the pH was further adjusted using 1 M NaOH solution. The swelling of carboxyl groups on the surface of the latex particles was deduced from the change in hydrodynamic particle diameter upon increasing pH of the serum.

2.3. Viscosity vs. shear rate measurement

Measurement of the viscosity, η, as a function of shear rate, $\dot{\gamma}$ was done using a rotational rheometer with 35-mm plate-plate geometry at three different pH of 4, 8 and 10 for all latexes. Samples with solids content ranging from 42 to 50 wt.% and an ionic strength of 10 and 100 mM were studied. The ionic strength of 10 mM was achieved by dialysis against distilled water. The dispersions with the electrolyte level of 100 mM were prepared by an addition of a concentrated NaCl solution into the latex dispersions. All viscosity measurements were done in the controlled

stress mode with the stress varying from 0.2 to 100 Pa within 300 s.

The changes of hydrodynamic particle size with pH could be obtained directly from the zero shear viscosity data according to the classical Quemada equation [16]:

$$\eta_0 = \mu_0\left[1 - \frac{\phi_{eff}}{\phi_{max}}\right]^{-2} \quad (1)$$

where η_0 is the zero shear viscosity and the μ_0 is the viscosity of the aqueous phase. ϕ_{eff} is the effective particle volume fraction which includes the dissociated carboxyl groups on the surface as a hairy layer. The zero shear viscosity diverges at a concentration ϕ_{max}, which for colloidal hard sphere dispersions is controlled by the so-called colloidal glass transition, ϕ_{glass}. As the particle concentration increases, their mobility reduces and finally they are trapped in a cage provided by surrounding particles, which prevents long range motion and results in a divergence of the zero shear viscosity at a particle concentration, $\phi_{glass} = 0.58$ [17]. This concentration is significantly below the random close packing, $\phi_{rcp} = 0.64$, which is often identified with ϕ_{max}.

With the adsorbed co-monomers on the surface of latex particles, the volume fraction of the core particle, ϕ is related to the effective volume fraction, ϕ_{eff} according to:

$$\phi_{eff} = \phi\left(1 + \frac{\delta}{a}\right)^3 \quad (2)$$

where δ is the length of the hairy layer, and a is the core radius of the particle which is obtained by dynamic light scattering at pH = 3, here the change of δ is based on the reference value at this low pH. Using Eqs. (1) and (2) the hairy particles are thus treated as hard spheres with an increased particle radius and volume (so-called hard-sphere mapping). We demonstrate the validity of using the Quemada equation and the hard-sphere mapping concept studying the dependence of the zero shear viscosity on particle loading for one of our latex system (styrene–butylacrylate latex functionalized with itaconic acid). Fig. 2 clearly shows that these data can be fitted with Quemada's model using the exponent, $\alpha = -2$, $\phi_{max} = 0.58$, and $\phi_{eff} = \phi$, *i.e.* of $\delta = 0$ nm. The exponent, $\alpha = -2.55$ suggested by mode coupling theory [18] for the divergence of η_0 close to the glass transition is not appropriate in the concentration range investigated here. Nevertheless, $\phi_{max} = \phi_{glass}$ should be chosen, setting ϕ_{max} equal to ϕ_{rcp} would result in higher δ values in all cases investigated here. For the IA-systems shown in Fig. 2, $\phi_{max} = \phi_{rcp}$ would lead to $\delta = 2$ nm. This gives a confidence range for the determination of δ and we conclude that we can determine this quantity with an experimental error of ±1 nm.

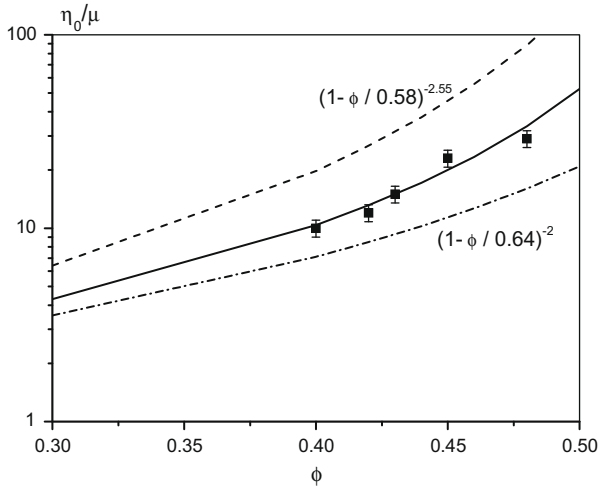

Fig. 2. The relative zero shear viscosity as a function of particle volume fraction with the data plotted for styrene–butylacrylate latex copolymerized with itaconic acid as a functional co-monomer. Solid line follows Quemada's equation (Eq. (1)) with $\phi_{eff} = \phi$. Dashed lines are calculated using either $\phi_{max} = \phi_{rcp} = 0.64$ and exponent of −2.55 as indicated in the graph.

2.4. High frequency rheology using torsional resonators

We have used two torsional resonators operating at the frequencies of 19, 58 kHz (cylinder-type) and 8, 31 kHz (dumbbell-type) in order to determine the linear viscoelastic moduli G' and G'' in the high frequency range (Fig. 3). The temperature for all measurements was controlled by a thermostat device connected to the resonators within ±0.01 °C. Upon immersion of the resonator in a liquid its resonance frequency decreases and the width of the resonance curve increases compared to the free oscillation in air. The resonance frequency, f and the width of the resonance curve, D are measured using a lock-in amplifier. The difference between values for free (f_{Air}, D_{Air}) and loaded (f_{Sample}, D_{Sample}) oscillation, $\Delta f = f_{Sample} - f_{Air}$ and $\Delta D = D_{Sample} - D_{Air}$, is then used to calculate the rheological quantities G' (storage modulus) and G'' (loss modulus) as follows [15]:

$$G' = \frac{k}{\rho}\left[\left(\frac{\Delta D}{2}\right)^2 - \Delta f^2 + \frac{2c\Delta D\Delta f}{1+c^2}\right] + d \quad (3)$$

$$G'' = \frac{k}{\rho}\left\{-\Delta D\Delta f + \frac{2c}{1+c^2}\left[\left(\frac{\Delta D}{2}\right)^2 - \Delta f^2\right]\right\} \quad (4)$$

where ρ is the fluid density and k, c, and d are instrument constants. For the resonators used here d is set to be zero, and k and c are obtained by calibration with a series of silicon oils: AK 5, AK 10, AK 50, AK 100, AK 200, and AK 500. These fluids cover a viscosity range from 5 mPa s to 500 mPa s. It should be noted, that the viscosity range covered here is expanded to higher values compared to the calibration presented by Fritz et al. [15]. At low shear rates or oscillation frequencies the fluids used here behave Newtonian, but in the high frequency range, especially the higher viscosity grade silicon oils exhibit significant viscoelasticity. Therefore, the calibration procedure has to account for G' as well as G''. This is different from the previous calibration assuming purely Newtonian behavior of the calibration liquids.

The requested high frequency values for G' and G'' were determined as follows: since the analyzed silicon oils are un-entangled (as their molecular-weight is below the critical molecular-weight for entanglements of 24,000 g/mol), their relaxation behavior is well described by the classical Rouse model [19]. Respective G' and G'' data have been measured in the frequency range up to 10 kHz using an oscillatory squeeze flow device [20]. Then the Rouse model was fitted to these experimental data and finally the values relevant for the resonators were extrapolated as shown for AK 200 in Fig. 4.

Consequently, the values of k and c were then obtained by minimizing the difference, Δ, between measured and calculated (as described above) values for G' and G'' for the $N = 6$ silicon oils simultaneously by:

$$\Delta = \sqrt{\frac{1}{N}\left[\sum_{i=1}^{N}\left(\frac{\eta'_{expt,i} - \eta'_{calc,i}}{\eta'_{calc,i}}\right)^2 + \sum_{i=1}^{N}\left(\frac{\eta''_{expt,i} - \eta''_{calc,i}}{\eta''_{calc,i}}\right)^2\right]} \quad (5)$$

Here we use the complex viscosity $\eta^* = \eta' - \eta''$ which is related to $G^* = G' + iG''$ according to $\eta' = G''/\omega$ and $\eta'' = G'/\omega$.

The high frequency viscosity, η'_∞ for suspensions of hard spheres is solely controlled by particle loading. Lionberger and

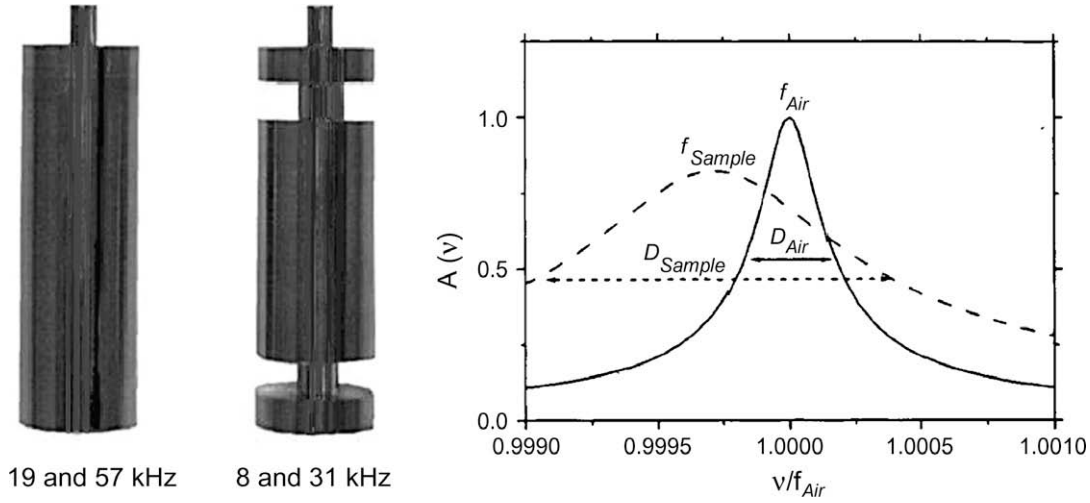

Fig. 3. High frequency torsional resonators operated at different frequencies in the range 8–57 kHz. The diagram on the right hand side shows the oscillation amplitude normalized to its maximum value $A(\nu = f_{Air})$. The rheological properties are calculated for the difference of measured values for the free (f_{Air}, D_{Air}) and the loaded (f_{Sample}, D_{Sample}) resonator.

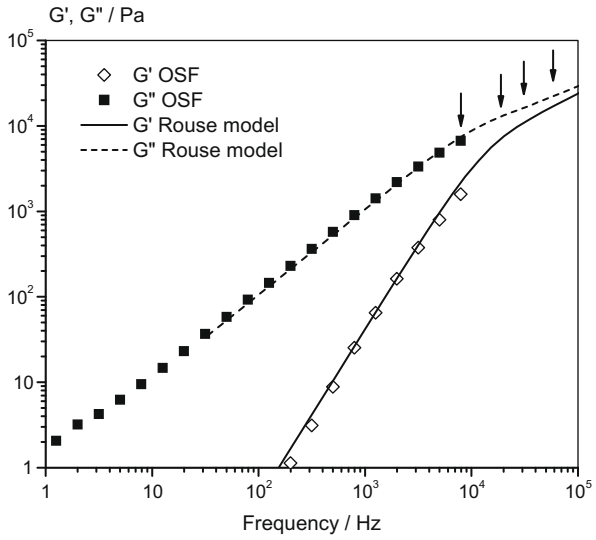

Fig. 4. The elastic and loss modulus, G' and G'' for silicon oil AK 200, fit of the Rouse model (lines) to the experimental data from oscillatory squeeze flow, OSF (symbols). The arrows indicate the resonance frequencies of the torsional resonators used here.

Russel [21] have provided a semi-empirical model relating $\eta'_\infty = \lim_{\omega\to\infty} \eta'$ and volume fraction ϕ.

$$\frac{\eta'_\infty}{\mu_0} = \frac{1 + \frac{3}{2}\phi_{eff}\left(1 + \phi_{eff} - 0.189\phi_{eff}^2\right)}{1 - \phi_{eff}\left(1 + \phi_{eff} - 0.189\phi_{eff}^2\right)} \quad (6)$$

This relationship is used here to determine ϕ_{eff} and then δ using Eq. (2).

3. Results and discussion

DLS results are summarized in Table 1. It should be carefully noted that the thickness of "hairy" surface layer reported in the table is relative to the reference value at pH = 3. Therefore, no changes of the δ values at pH = 4 for SA–IA and SA–AM does not mean that there is absolutely no "hairy" layer on the surface. The carboxyl groups of itaconic acid can dissociate even at pH less than 3. Acrylamide functionalized latex exhibits the presence of a thin hairy layer independent of pH as will be discussed below. Furthermore, the thickness of the collapsed functional group layer on the particle surface can be estimated to be ≈0.5 nm assuming that all functional monomers are densely packed on the particle surface.

Table 1
Thickness of hairy layer, δ (nm) obtained from dynamic light scattering (DLS), steady shear (SS) and high frequency (HF) technique for the styrene–butylacrylate latexes with an ionic strength of 10 mM. The confidence range is ±1 nm for all data.

Latexes/pH	4			8			10		
	DLS	SS	HF	DLS	SS	HF	DLS	SS	HF
SA–AA	1	1	1	3	2	2	4	3	3
SA–MAA	0	0	0	1	1	1	2	2	2
SA–IA	0	0	1	1	1	1	1	1	1

Fig. 5 presents the viscosity data against shear rate using steady shear measurement for a carboxylated styrene–butylacrylate latex

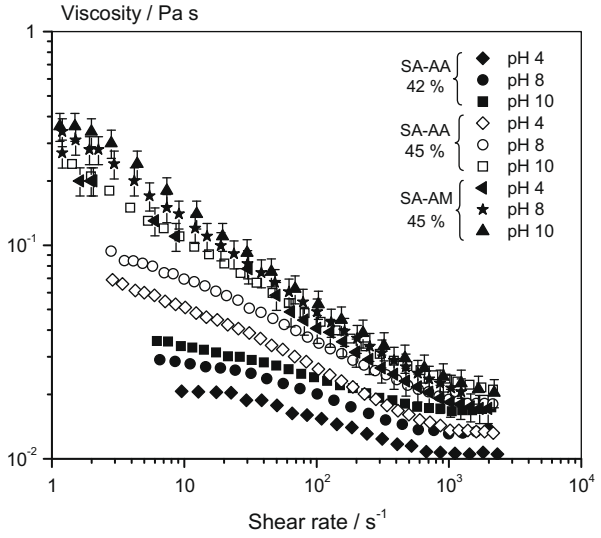

Fig. 5. The pH dependence of viscosity as a function of shear rate for styrene–butylacrylate with acrylic acid or acrylamide as a co-monomer. Solids content as shown in the figure, ionic strength: 10 mM.

with acrylic acid as functional co-monomer. Data are shown for 42 and 45 wt.% particle loading at pH values of 4, 8 and 10. We observe a monotonic increase of viscosity as pH increases from 4 to 10 as expected due to dissociation of acrylic acid on the particle surface. At 42% solids content a plateau is clearly seen in the low shear limit, which refers to the zero shear viscosity, η_0. The thickness of the surface layer has been extracted using Quemada equation (Eqs. (1) and (2)) and the results of these calculations are also included in Table 1.

In Fig. 5, viscosity data vs. shear rate are also shown for the styrene–butylacrylate latex with acrylamide as a functional co-monomer. In contrast to the results of acrylic acid functionalized latex discussed above, the viscosity of acrylamide based latex is insensitive to the pH within experimental error, as expected since acrylamide is an electrically neutral monomer, i.e. there is no dissociation of surface charge groups, however, this does not mean that there is no "hair" on the particle surface. A first indication for the existence of a protective surface layer is, that the pH of the latex could be adjusted by an addition of concentrated 10 M NaOH solution without observable local coagulation. On the other hand, it is clearly seen, that the absolute value of the viscosity is significantly higher for the SA–AM latex than for the SA–AA latex compared at similar particle loading. The zero shear viscosity if it exists at all is not reached in the shear rate range investigated here, but we can take the highest viscosity value measured as a lower boundary for η_0, but then application of Quemada's equation would lead to unphysically high values of ϕ_{eff} indicating that the simple concept of hard-sphere mapping does not apply and we do not calculate a hairy layer thickness, δ for the SA–AM latex. The reason for this will be discussed below in the context of the high frequency rheology results.

The high frequency rheological measurement were carried out for styrene–butylacrylate latexes functionalized with different co-monomers on the surface as discussed earlier in the experimental section. Fig. 6 represents the high frequency viscosity, η' vs. ω for latexes copolymerized with acrylic acid and acrylamide, respectively. In analogy to the steady shear viscosity (Fig. 5), the high frequency viscosity increases with an increase of pH in the case of acrylic acid, and no significant pH dependence of η' is observed with acrylamide. The slight decrease of high frequency viscosity with ω is typical for "hairy particles" due to the permeability of hairy surface layer [22]. However, we also observe a decrease of high frequency viscosity vs. ω for the AM functionalized latex and the absolute values for η' are similar to that for the SA–AA latex at pH = 4, therefore we conclude, that there is a thin hairy layer or swollen particle surface of about 1 nm, also for the SA–AM latex, which is attributed to the hydrophilicity of the acrylamide groups. Obviously, high frequency viscosity measurements are more sensitive to such subtle surface modifications than DLS data. The low δ value in the AM case is either due to the low solubility of the AM similar to the non-dissociated acid groups or it is due to a preferred polymerization of AM in the aqueous phase as shown by Kawaguchi et al. [2].

Fig. 7 shows how the serum pH affects the high frequency elastic modulus, G' of acrylic acid functionalized latex. By increasing the pH from 4 to 10, it is observed that the elastic modulus increases monotonically as a result of the dissociation of carboxyl groups on the particle surface. Fig. 7 also shows the elastic modulus, G' for acrylamide functionalized latex. In contrast to the acrylic acid based latex, we do not observe a change of G' with pH, since acrylamide has no charge on the surface as mentioned above. Nevertheless, the absolute value of G' is higher for the AM functionalized latex than for the one copolymerized with AA. This directly reveals that the colloidal interaction among particles is stronger in the AM case than in the AA case. This is important information complementary to the thickness of the hairy layer. While the range of the steric interaction is determined by δ, its strength depends on the density of the monomer units in the hairy layer and on the solvent quality of the liquid phase usually expressed in terms of the Flory Huggins mixing parameter χ [23]. In a poor solvent the steric interaction due to a hairy surface layer can even be attractive. High frequency viscosity measurements, which are solely determined by the effective particle volume fraction, ϕ_{eff}, clearly show that the particles copolymerized with AM do not form extended hairy surface layers. Therefore, we conclude, that the total interaction, which is the sum of the steric repulsion and van der Waals attraction exhibits a minimum as schematically sketched in Fig. 8. The interaction energy between acrylamide functionalized latex particles has also been estimated using a model for the steric interaction valid in the limit of thin hairy surface layers with constant monomer density proposed by Vincent and coworkers [12,24].

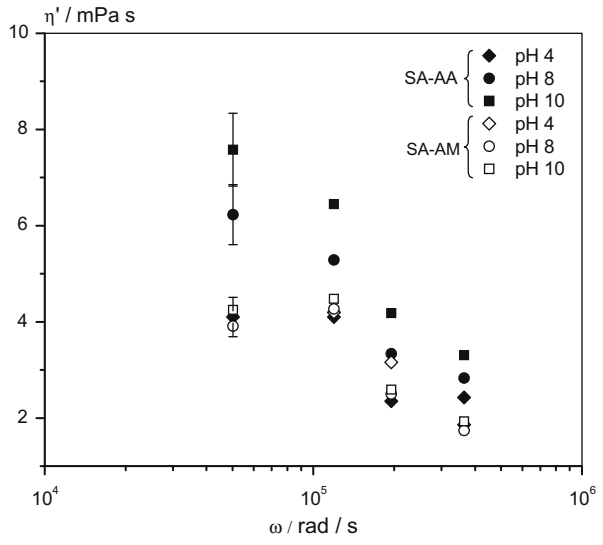

Fig. 6. High frequency viscosity, η' as a function of angular frequency, ω for styrene–butylacrylate with acrylic acid or acrylamide as a co-monomer. Solids content: 45%, ionic strength: 10 mM.

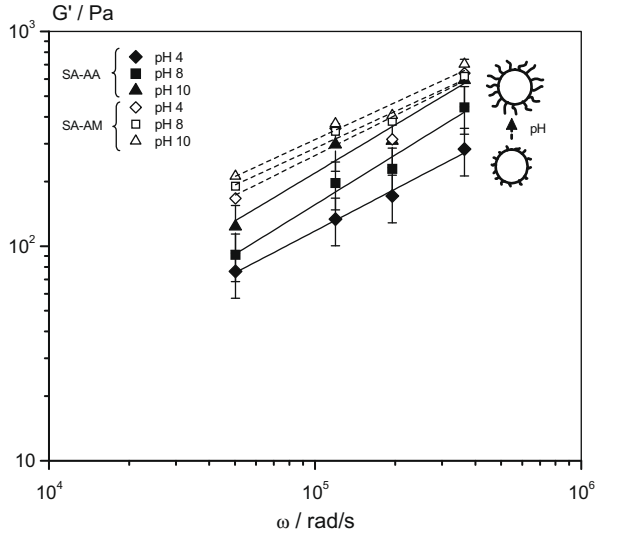

Fig. 7. Elastic modulus with pH variation for acrylic acid functionalized styrene–butylacrylate (SA–AA) latex showing swelling of the hairy layer as the serum pH increases (filled symbols) and acrylamide functionalized styrene–butylacrylate latex (SA–AM) showing no swelling of surface layer (opened symbols). Latex solids content: 45%, ionic strength: 10 mM.

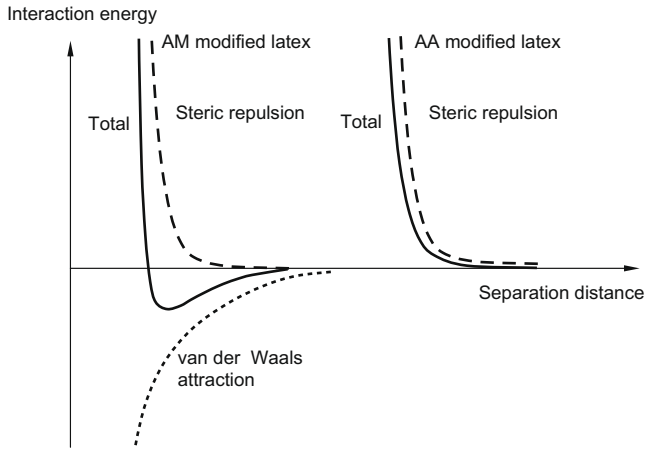

Fig. 8. Interaction energy vs. separation distance between two particles. Schematic sketch of the difference between the AA- and AM-functionalized latexes.

The electrostatic contribution to the interaction potential due to a small fraction of sulfate groups from the initiator is neglected and the total interaction energy (V_T) is the combination of attractive van der Waals, V_{vdw} and repulsive steric interactions, V_{str} as follows:

$$V_T = V_{vdw} + V_{str} \tag{7}$$

$$\frac{V_{vdw}}{kT} = -\frac{A}{6kT}\left[\frac{2a^2}{H(4a+H)} + \frac{2a^2}{(2a+H)^2} + \ln\frac{H(4a+H)}{(2a+H)^2}\right] \tag{8}$$

$$\frac{V_{str}}{kT} = 0 \quad 2L \leqslant H$$

$$\frac{V_{str}}{kT} = \frac{4\pi a}{v_1}\phi_p^2\left(\frac{1}{2}-\chi\right)\left(L-\frac{H}{2}\right)^2 \quad L \leqslant H < 2L$$

$$\frac{V_{str}}{kT} = \frac{4\pi a}{v_1}\phi_p^2\left(\frac{1}{2}-\chi\right)L^2\left(\frac{H}{2L}-\frac{1}{4}-\ln\left(\frac{H}{L}\right)\right) \quad H < L \tag{9}$$

where A is the Hamaker constant, H is the surface-to-surface distance between particles, χ is the Flory–Huggins solvency parameter, ϕ_p is the volume fraction of acrylamide within the layer, L is the surface layer thickness, v_1 is the volume of one solvent molecule and a represents the core radius of the particles. Using the Hamaker constant of polystyrene $A \sim 2.2 \times 10^{-20}$ J [23], Flory Huggins solvency parameter, $\chi \sim 0.41$ [25], assuming a volume fraction of acrylamide within the layer of 0.50 and taking the thickness of the surface layer of 1 nm, results in a secondary minimum in V_T with a depth of around 10 kT at about 2 nm surface-to-surface separation distance between particles. Consequently, we conclude that the presence of an interaction energy minimum leads to a weak, reversible aggregation of particles, which accounts for the high low shear viscosity of the SA–AM latex compared to the other systems functionalized by different acid groups. So in the light of these high frequency rheology experiments, it is not appropriate to determine δ from η_0 data in this case as already stated above. It should be noted, that this aggregation does not lead to irreversible large scale coagulation. Instead, the dispersion is stable for at least 6 months and it easily flows if exposed to external shear forces. There is no indication of a weak aggregation in the case of the IA-modified latex, which has a similarly thin hairy layer and we attribute this to the additional contribution of the electrostatic repulsion due to the dissociated acid groups. It is also well-known that the high frequency modulus can be related to the colloidal particle interactions, and it has been used extensively for repulsive as well as hard sphere systems [12–15,20–22,26]. For our electrostatically stabilized repulsive latexes investigated here, the high frequency modulus follows the expected trends as pH and volume fraction are varied. For AM-modified latex, an unexpected high G' modulus was found independent of pH, and in the light of the viscosity and DLS data, it is adequate to interpret this as a signature of attractive particle interaction, but unfortunately there is no statistical mechanical theory available for further data analysis.

Fig. 7 also shows, that the frequency dependence of elastic modulus can be estimated by a power-law: $G' \sim \omega^{\alpha}$. The results of all exponents, α are summarized in Table 2 and 3 for the case of ionic strength of 10 and 100 mM, respectively. The exponent is related to the particle interaction [15], e.g., for charge stabilized systems $\alpha = 0$ and for hard sphere suspensions $\alpha = 0.5$ [21,26]. For electrosterically stabilized systems, the scaling exponents of $0 < \alpha < 0.5$ have been reported [21]. The values for α obtained here mostly lie in the range of ~0.5–0.7. This indicates that our latexes behave very close to hard sphere particles despite of their functionalization. It should be kept in mind, that not all acid monomers used in the polymerization are located on the particle surface, they are partly present inside the particles or in the serum phase. Also, the amount of the acid groups adsorbed to the particle surface has possibly been reduced in the stage of dialysis.

The reason for the large values for $\alpha > 0.5$ is not yet really clear. There is no systematic change of α with pH or variation of co-monomer and particularly for the systems SA–AM and SA–IA, which should be close to hard sphere systems, there is no rationalization of these results. We are not aware of any theory predicting such large scaling exponents.

Fig. 9 compares the results for the thickness of the surface layer from three different techniques, i.e. high frequency (HF), steady shear (SS) and dynamic light scattering (DLS), respectively when introducing different co-monomers on the particle surface. It is observed that all techniques yield similar results. However, in general the high frequency viscosity measurement is of advantage over DLS, since the hydrodynamic particle size obtained from DLS measurement is based on unperturbed diffusivity of the particles, thus DLS has to be performed in very dilute stage, whereas viscosity measurements are done with concentrated dispersions. On the other hand, the high frequency viscosity, η' from which the hair length information is deduced is independent of colloidal interactions, which show up in the elasticity term, G'. Therefore, the interpretation of η' and the determination of ϕ_{eff} is straight forward and in addition, G' measurements yield supplementary information about particle–particle interactions. In contrast, the zero shear viscosity is determined by Brownian motion, hydrodynamic, as well

Table 2
A table summarizes of all scaling exponent from G' vs. ω with ionic strength of 10 mM. Solids content: 45%. The relative error is ±15% for all data.

Latexes/pH	4	8	10
SA–AA	0.65	0.76	0.75
SA–MAA	0.79	0.66	0.69
SA–IA	0.62	0.57	0.57
SA–AM	0.78	0.72	0.62
SB–AA	0.72	0.73	0.45
SB–AM	0.48	0.62	0.62
SB–IA	0.69	0.79	0.81

Table 3
A table summarizes of all scaling exponent from G' vs. ω with ionic strength of 100 mM. Solids content: 45%. The relative error is ±15% for all data.

Latexes/pH	4	8	10
SA–AA	0.67	0.83	0.72
SA–MAA	0.52	0.84	0.49
SA–IA	0.66	0.50	0.51
SA–AM	0.45	0.43	0.59

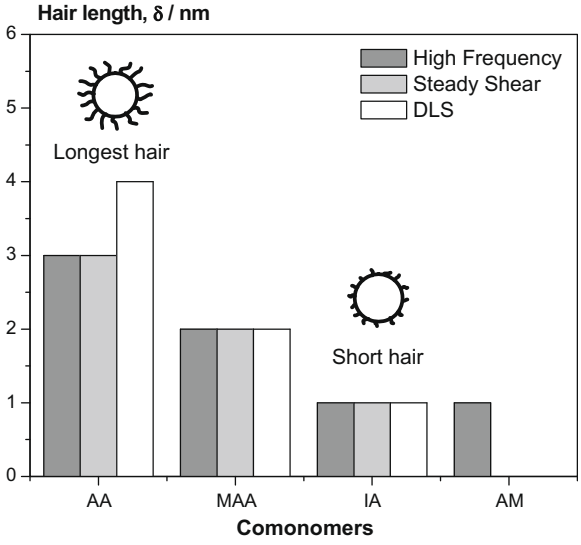

Fig. 9. Thickness of the surface layer of styrene–butylacrylate latex functionalized with acrylic acid (AA), methacrylic acid (MAA) and itaconic acid (IA) as well as acrylamide (AM). The hair lengths, δ shown are obtained using three different methods, i.e. high frequency, steady shear and dynamic light scattering (DLS) measurements. Latex solids content: 45%, pH = 10, and ionic strength: 10 mM. Note, DLS gives only changes in δ relative to the reference state at pH = 3. High frequency and steady shear data are based on a hard-sphere mapping providing ϕ_{eff} and then δ according to Eq. (2). This approach is not valid for the steady shear data of the AM-latex.

as colloidal interactions. The contributions from these phenomena are hard to separate and a simple hard-sphere mapping and determination of ϕ_{eff} and δ from Eqs. (1) and (2) can lead to erroneous results as shown here for the AM-modified latexes.

The high frequency rheological measurements were also done for the latexes with other functional co-monomers, i.e. methacrylic and itaconic acids. The effect of these functional groups on the high frequency viscosity, η' is now summarized in Fig. 10, where η' evaluated at the highest frequency accessible f_{max} = 57 kHz is plotted against pH. When the carboxyl groups dissociate, it results in an increase of particle effective volume, therefore the high frequency

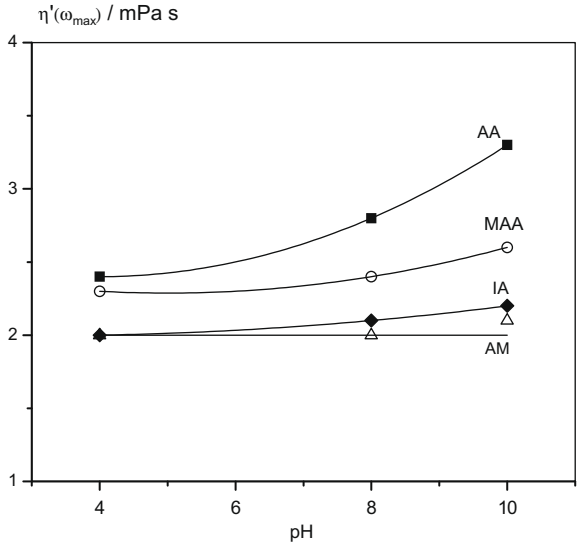

Fig. 10. High frequency viscosity with pH variation obtained at, $\omega_{max} = (2\pi) \cdot 57$ kHz for acrylic (AA), methacrylic (MAA) and itaconic acid (IA) as well as acrylamide (AM). Latex solid contents content: 45% and ionic strength: 10 mM.

viscosity is expected to increase with increasing pH. Generally, these results agree very well with those from DLS and steady shear viscosity measurements. It is clearly seen that at pH above neutral, the acrylic acid functionalized latex has the strongest increase in effective volume fraction, i.e. the most extended hairy surface layer among the latexes investigated here. Our results are rationalized as follows: the acrylic acid copolymerizes with other monomers, i.e., butadiene, buthylacrylate (BA), etc. and tends to make random copolymers, therefore there would be a chain AA-BA-BA-AA-BA-AA-BA-attaching on the latex surface. This makes the acrylic acid easier to extend [1,27]. A direct proof of hairy layer in the acrylic acid case is shown in Fig. 11, where Fig. 11a and b depicts the electron micrograph images of dried latex film for pH = 4 and 10, respectively. The films were stained with uranyl acetate for proper image contrast. It is clearly seen that the formation of hairy layers around particles is more pronounced at high pH. The methacrylic acid is more hydrophobic than acrylic acid, so it tends to go inside of the particle [27], which results in a thinner "hairy" surface layer compared to the AA case.

In contrast, the swelling of itaconic acid based latex is relatively small at high pH compared to other acid groups, since itaconic acid terminates the polymer chain, so only one IA attaches at the particle surface. This makes very dense charge groups on the surface but, however cannot stretch out. This also limits the hairy layer if itaconic acid to less than 2 nm thickness. The acrylamide functionalized latex is insensitive to the pH changes as already discussed above.

No significant difference in the rheological properties was found when styrene–butylacrylate and styrene–butadiene latexes were studied with the same functionalization.

3.1. Effect of ionic strength of the serum

To study the effect of ionic strength of the serum, additional high frequency viscosity measurement was carried out for an ionic strength of 100 mM. The thickness of the hairy layer, δ calculated from Eq. (6) reduces from 3 nm to 2 nm for acrylic acid and from 2 to 1 nm for methacrylic acid upon increasing ionic strength from 10 to 100 mM. The itaconic and acrylamide based latexes show no significant effect on the ionic strength, particularly the itaconic acid based latex has relatively short and dense hair while the acrylamide based latex has no surface charged groups. From these results we find an expected shrinkage of the hairy layer upon increasing the serum ionic strength, basically for those latexes with an extended hairy layer like acrylic and methacrylic acid.

3.2. Effect of temperature

We have investigated the temperature dependence of the rheology of all four functionalized latexes performing steady shear viscosity as well as high frequency modulus measurements at 20, 40 and 60 °C using solid contents of 40 wt.% and pH = 10. In Fig. 12 we display the relative zero shear viscosity, η_0/μ_0, normalized to the solvent viscosity in order to account for the effect of temperature, as well as the elastic modulus, G' obtained at the highest accessible frequency, $\omega_{max} = (2\pi) \cdot 57$ kHz as a function of temperature. Obviously, both quantities do not change with temperature in the range investigated here. Therefore, we conclude, that the "hairy" surface layer and the colloidal interactions among particles also do not alter significantly upon variation of temperature.

4. Conclusion

Dynamic light scattering, steady shear and high frequency viscosity measurements have been used to characterize the surface

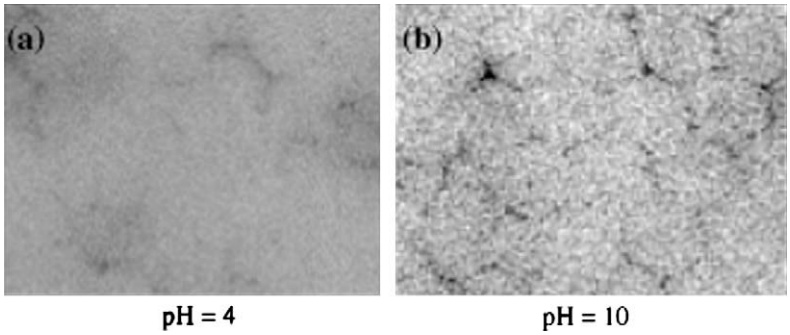

Fig. 11. Electron micrograph of films formed from SA–AA dispersion at pH 4 and 10.

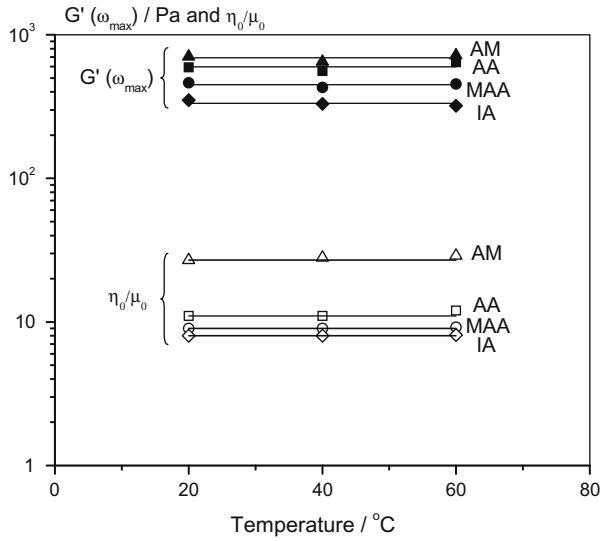

Fig. 12. Relative low shear viscosity, η_0/μ_0 and the elastic modulus, G' (evaluated at ω_{max}) for styrene–butylacrylate latex functionalized with acrylic acid (AA), methacrylic acid (MAA), itaconic acid (IA) and acrylamide (AM) at pH = 10 and ionic strength: 10 mM, latex solids content: 40% (viscosity data) and 45% (modulus data).

layer thickness, δ of carboxylated latex particles. We compare the results obtained from these methods and conclude that these techniques provide consistent and complementary results. The benefit of using high frequency rheology is that it is done at high concentrations relevant for manufacturing and application of such dispersions and that it provides additional information about type and strength of colloidal interactions.

We analyzed the effect of different co-monomers including acrylic acid, methacrylic acid and itaconic acid as well as the electrically neutral acrylamide on the formation of hairy layer and found that the acrylic acid copolymerized latex is very sensitive to the pH and ionic strength with acrylic acid expands to 3–4 nm by increasing the pH from 4 to 10 while methacrylic functionalized latex shows shorter hair of less than 3 nm. The difference is attributed to a stronger hydrophobicity of MAA compared to AA and a corresponding higher tendency to polymerize inside the latex particles. Itaconic acid based latexes have relatively short hairs of below 2 nm even at pH = 10, this can be rationalized by the fact that IA terminates the polymerization and thus cannot form extended chain sequences swollen in the aqueous phase. In contrast, the latexes with acrylamide are insensitive variation of pH. However they have high viscosity values even at low pH. Together with the high G' and the low η' values obtained in high frequency measurements, this leads to the conclusion that the AM-functionalized latexes are weakly flocculated since there is no electrostatic repulsion among particles, the AM layer is not extended enough to balance van der Waals attraction. Nevertheless, AM provides a protective surface layer preventing irreversible coagulation.

Shrinkage of the hairy layer was found upon increasing the background ionic strength from 10 to 100 mM. Of around 33% decrease in the hairy layer thickness was observed for acrylic acid functionalized latex and ~50% decrease for methacrylic functionalized latex. But as expected, there is no effect on the hairy layer thickness for itaconic and acrylamide based latexes.

No significant difference in hairy layer thickness and rheological properties was found between styrene–butylacrylate and styrene–butadiene latexes when comparing samples with similar functionalization. Moreover, steady shear and high frequency rheology do not indicate any significant effect of temperature on hairy layer thickness and latex stability within the investigated temperature range 20 °C < T < 60 °C.

Acknowledgments

The authors thank Dr. Walter Heckmann from BASF SE Ludwigshafen, Germany for electron micrographs. The financial support from BASF Corporation, USA is gratefully acknowledged.

References

[1] B.W. Greene, J. Colloid Interface Sci. 43 (1973) 449.
[2] H. Kawakuchi, Y. Sugi, Y. Ohtsuka, J. Appl. Polym. Sci. 26 (1981) 1649.
[3] G.L. Shoaf, G.W. Poehlein, J. Appl. Polym. Sci. 42 (1991) 1213.
[4] G.L. Shoaf, G.W. Poehlein, J. Appl. Polym. Sci. 42 (1991) 1239.
[5] L. Vorwerg, R.G. Gilbert, Macromolecules 33 (2000) 6693.
[6] A. Zosel, W. Heckman, G. Ley, W. Mächtle, Colloid Polym. Sci. 265 (1987) 113.
[7] J.L. Ortega-Venuesa, A. Martin-Rodriguez, R. Hidalgo-Alvarez, J. Colloid Interface Sci. 184 (1996) 259.
[8] M.S. Romero-Cano, A. Martin-Rodriguez, F.J. de las Nieves, Langmuir 17 (2001) 3505.
[9] X.E.E. Reynhout, L. Hoekstra, J. Meuldijk, A.A.H. Drinkenburg, J. Polym. Sci., Part A: Polym. Chem. 41 (2003) 2985.
[10] X. Guo, M. Ballauff, Langmuir 16 (2000) 8719.
[11] X. Guo, M. Ballauff, Phys. Rev. E 64 (2001) 051406.
[12] G. Fritz, V. Schädler, N. Willenbacher, N.J. Wagner, Langmuir 18 (2002) 6381.
[13] J. Bergenholtz, N. Willenbacher, N.J. Wagner, B. Morrison, D. Van den Ende, J. Mellema, B. Morrison, J. Colloid Interface Sci. 202 (1998) 430.
[14] S.L. Elliot, W.B. Russel, J. Rheol. 42 (1998) 361.
[15] G. Fritz, W. Pechhold, N. Willenbacher, N. Wagner, J. Rheol. 47 (2003) 303.
[16] D. Quemada, Rheol. Acta 16 (1977) 82.
[17] W. Van Megan, S.M. Underwood, Phys. Rev. E 49 (1994) 4206.
[18] W. Petry, E. Bartsch, F. Fujara, M. Kiebel, H. Sillescu, B. Farago, Condens. Matter 83 (1991) 175.
[19] J.C. Ferry, Viscoelastic Properties of Polymers, third ed., Wiley, 1980.
[20] J. Crassous, R. Régisser, M. Ballauff, N. Willenbacher, J. Rheol. 49 (2005) 851.
[21] R.A. Lionberger, W.B. Russel, J. Rheol. 38 (1994) 1885.
[22] I. Deike, M. Ballauff, N. Willenbacher, A. Weiss, J. Rheol. 45 (2001) 709.
[23] P.C. Hiemenz, R. Rajagopalan, Principles of Colloid and Surface Chemistry, third ed., Marcel Dekker, New York, 1997. p. 125.
[24] B. Vincent, J. Edwards, S. Emment, A. Jones, Colloids Surf. 18 (1986) 261.
[25] F. Horkay, I. Tasaki, P.J. Basser, Biomacromolecules 1 (2000) 84.
[26] G. Fritz, B.J. Maranzano, N.J. Wagner, N. Willenbacher, J. Non-Newtonian Fluid Mech. 102 (2002) 149.
[27] A.M.d. Santos, T.F. McKenna, J. Guillot, J. Appl. Polym. Sci. 65 (1997).